Experimental investigation of forced-convection in a finned rhombic tube of the flat-plate solar collectors

Taherian, Hessam; Yazdanshenas, Eshagh

Published in:
Proceedings of the Second International Green Energy Conference

Publication date:
2006

Document Version
Publisher's PDF, also known as Version of record

Link back to DTU Orbit

Citation (APA):
Taherian, H., & Yazdanshenas, E. (2006). Experimental investigation of forced-convection in a finned rhombic tube of the flat-plate solar collectors. In *Proceedings of the Second International Green Energy Conference* (Vol. IGEC2-126, pp. 314-321)

EXPERIMENTAL INVESTIGATION OF FORCED-CONVECTION IN A FINNED RHOMBIC TUBE OF FLAT-PLATE SOLAR COLLECTORS

Hessam Taherian, Eshagh Yazdanshenas
*, ° Faculty of Mechanical Engineering, University of Mazandaran, Babol, Iran
taherih@nit.ac.ir, eshaghyazdanshenas@yahoo.com

ABSTRACT
Due to scarcity of literature on forced-convection heat transfer in a solar collector with rhombic cross-section absorbing tubes, a series of experiments was arranged and conducted to determine heat transfer coefficient. In this study, a typical rhombic cross-section finned tube of flat-plate collectors used as the test section. Two correlations were proposed for the Nusselt number as a function of the Reynolds number and the Prandtl number based on hydraulic diameter for various heat fluxes. The temperature distribution along the finned tube for the fluid and the wall were also illustrated.

INTRODUCTION
Solar flat plate collectors are widely used in the world. They can be used for various purposes such as producing domestic hot water and preheating ventilation air through connection to the space heating system. According to statistics, up to 2001, 49% of the collector market in the world has been for traditional flat plate collectors. Due to extensive use of flat plate collectors, it entails to investigate on different types of them. Glazed flat-plate collectors are very common and are available as liquid-based and air-based collectors. These collectors are better suited for moderate temperature applications where the demand temperature is 30-70C and/or for applications that require heat during the winter months. The liquid-based collectors are most commonly used for heating of domestic and commercial hot water and indoor swimming pools. The air-based collectors are used for heating of buildings, ventilation air and crop drying.

Some researchers investigated flat plate collectors with different configurations. Some used several collectors and some employed a single collector. Duffie and Beckman, 1991 reported that flow distribution strongly affects the efficiency of flat plate collectors. Therefore, many researchers studied the uniformity of flow distribution in flat plate collectors to name a few Chiou ,1982, Jones and Lior ,1994. Weitbrecht et al., 2002 experimentally and analytically studied a z-configuration water flat plate collector with laminar flow condition to investigate its flow distribution. They found out the flow distribution depends on the relation between energy loss in the risers and the energy loss in the manifolds. They also suggested performing further experiments with the other geometries that seemed to be essential for collector design.

Fan et al., 2005 investigated flow and temperature distribution in a solar collector panel with horizontal fins numerically and experimentally. A 12.5 m^2 solar collector panel with 16 parallel-connected horizontal fins was used for their study. Their experiments and CFD simulations showed that CFD simulations are relatively good for high flow rates, but not for the lower flow rates. Their results showed, by increasing tilt angle and inlet flow temperature, the flow distribution became worse. This phenomenon is not as much of noteworthy for high flow rates.

Obtaining heat transfer coefficient is the most indispensable part of designing a flat plate collector. There are varieties of flat plate collectors with different cross-sections such as circular, rectangular, hexagonal, and rhombic. Sunstrip fins manufactured by Thermo Dynamics Ltd, which has a rhombic and cross section with round corners, are widely used in solar thermal systems. They offer advantages over other fins for instance, high thermal performance and light weight and high rigidity due to their construction.

The purpose of this study is to experiment on a single Sunstrip fin in order to determine the forced convection heat transfer coefficient for design purposes.

EXPERIMENTAL APPARATUS
Fig. 1 is a schematic of apparatus arranged for finned tube heat transfer experiments. The system consisted of an open loop. Water was used as the working fluid pumped into the tank and the test section by means of a hydraulic bench equipped with a submersible pump. The temperature of the inlet water was controlled by varying the supply voltage of a 220 V, 2500 W electric heater positioned in the tank. Two valves were used

at the entrance and exit ports of the open loop. The flow rates were controlled and varied by the outlet valve and was measured using a stopwatch and a measuring cylinder located at the outlet of the open loop.

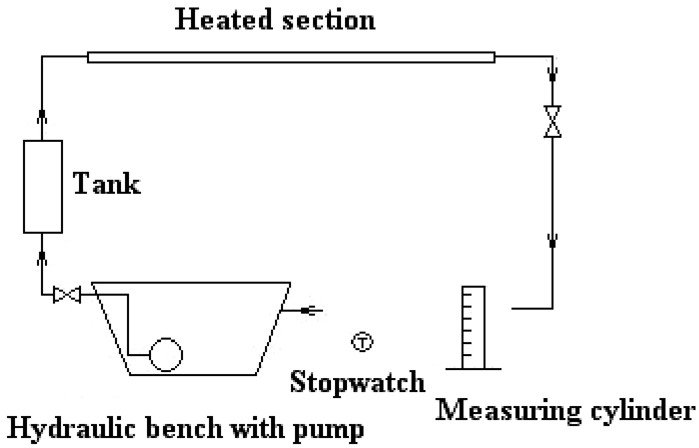

Fig. 1. Schematic diagram of the experimental apparatus

The test section consisted of single rhombic cross-section copper tubing with longitudinal aluminum fins on both sides as shown in Fig. 2. The fins are 0.5 mm thick and 7.15 cm wide. The length of the test section and the heated section was 1.75 m. The specification of the tube is shown in Fig. 2a. The hydraulic diameter was found to be 8.04 mm. The heat input was generated by 3.46 Ω / m electric heating wire. The eight-meter long heating wire was covered by a high temperature insulating varnish coating to prevent electrical contact between the heating wire and the fin plate. It was then positioned evenly in four parallel passes on the test section and was fixed on the plate by using small aluminum clips riveted to the fins to ensure that it stayed tightly and distributed the heat consistently. The input supply for heating wire was controlled by an electric dimmer. A 15-cm thick layer of glass wool thermal insulation covered the whole test section. Moreover, a thin aluminum foil was used to cover the entire area of insulation.

T-type (Cu-Const) thermocouples were used to obtain temperature distribution along the finned tube. 22 thermocouples were used for measuring the wall and fluid temperatures. Wall temperatures were measured at seven points along the finned tube and fluid temperatures were measured at eight points as shown in Fig. 2b. For wall temperatures, two thermocouples were soldered at the top and the bottom surface, respectively. Thermocouples used for fluid temperature was meticulously installed at the middle of the tube by using a high temperature glue. A number of preliminary tests were run to check and fix any problems.

A data acquisition system consisting of a PC and a Campbell Scientific datalogger model CR10X having six basic measurement channels was used to log the temperatures. The number of input channels was increased to 32 by using a relay multiplexer. All data were taken when the steady state condition was achieved. The data accumulated every 30 seconds. Moreover, the recorded values were stored and were averaged over a period of 10 minutes after reaching steady state.

The boundary condition is asymmetric due to the uniform heat flux at the top and the insulation at the bottom of the finned tube, which conforms to a real flat-plate collector.

Tests were performed at various inlet temperatures, heat fluxes and flow rates within the range of forced convection heat transfer.

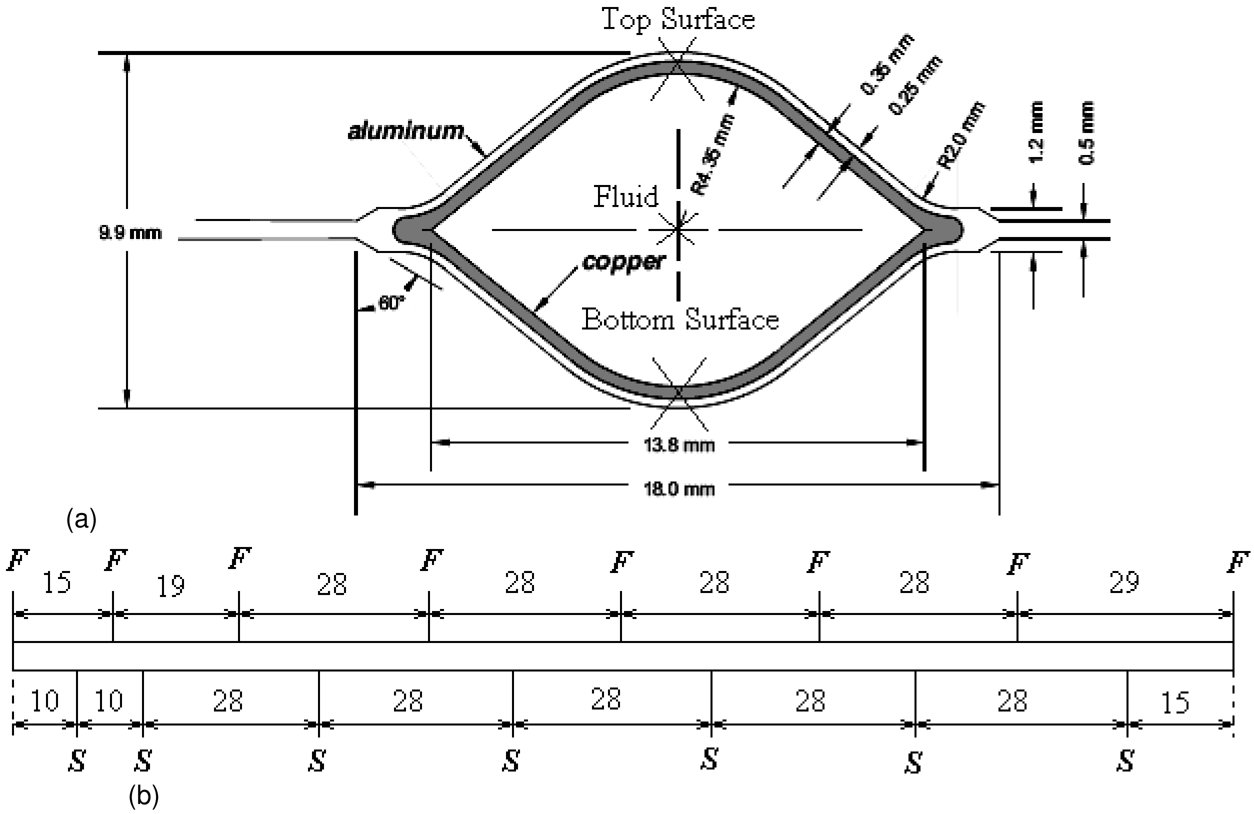

Fig. 2. Thermocouple locations in a cross-section and along the finned tube (dimension in cm)

The maximum uncertainty of temperature measurements was 0.3 $^{\circ}C$. The method of Kline and McClintok, 1953 was used to determine the level of uncertainty in calculating the important parameters from measured data. These uncertainties are tabulated in Table 1.

Table 1. Maximum experiment uncertainties

Parameter	Q	h	Nu_{D_h}	$\dot{m}$	V	Re_{D_h}
Uncertainty	3.7%	9.96%	9.95%	2.17%	2.4%	2.4%

RESULTS AND DISCUSSION

Nu-Re Correlation

First the heat rate is determined by Eq.(1). Here the surface temperature and the fluid temperatures were averaged over the periphery and the entire length of the tube. All properties were calculated at the average of the inlet and outlet fluid temperatures.

$$Q = \dot{m} C_p \left(T_{f,o} - T_{f,i} \right) \tag{1}$$

Heat transfer coefficient was obtained by Eq.(2).

$$h = \frac{Q}{A\left(T_{s,m} - T_{f,m}\right)} \tag{2}$$

As mentioned before, the flow rate was determined using a measuring cylinder and a stopwatch. By dividing the volume of collected water by the measured time, the flow rate was calculated. In addition, the mass flow rate was calculated by multiplying the flow rate by the average fluid density. The fluid velocity and the Reynolds number based on hydraulic diameter can be determined using Eq.(3) and Eq.(4), respectively.

$$V = \frac{\dot{m}}{\rho A_c} \tag{3}$$

$$\mathrm{Re}_{Dh} = \frac{\rho V D_h}{\mu} \tag{4}$$

The hydraulic diameter was defined as four times the cross-sectional area of the tube divided by the wetted perimeter.

A total of 51 tests were performed in this investigation covering Reynolds numbers from 290 to 7480 and Prandtl numbers from 2.77 to 6.53.

It can be noted from Fig. (3) that for low Reynolds numbers e.g. $\mathrm{Re} < 1000$, the Nusselt numbers range between about 19 and 21. Comparing the results with the fully developed forced convection Nusselt number reported by Sparrow and Haji-Sheikh, 1966 that is $Nu = 4.089$, the Nusselt number was found to be about five times higher than their results. In addition, as the Reynolds number increases beyond 1000, the Nusselt number increases more rapidly, which is attributed to turbulence.

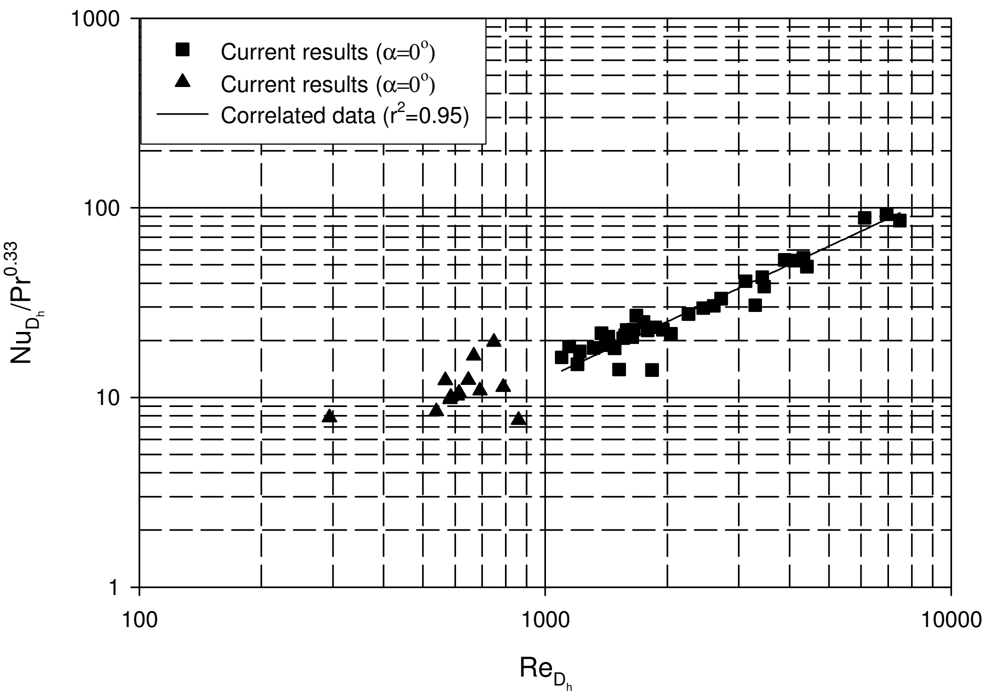

Fig. 3. The Nusselt number versus the Reynolds number

Eq.(5) was found to best fit the data for the range $\mathrm{Re} > 1000$ having a correlation coefficient $r^2 = 0.95$.

$$Nu_{D_h} = 0.0127\,\mathrm{Re}_{D_h}{}^{0.998}\,\mathrm{Pr}^{0.33}, \qquad \begin{cases} 1000 < \mathrm{Re} < 7840 \\ 2.77 < \mathrm{Pr} < 6.5 \\ \alpha = 0^\circ \end{cases} \tag{5}$$

The proposed correlation is useful for design of flat plate solar collectors with rhombic cross-section tubes and it is valid for $1000 < \mathrm{Re} < 7840$.

In order to propose a unique correlation for the low Reynolds number, the Reynolds number with the Prandtl number was chosen as the independent parameters. Fig. 4 is the diagram of the Nusselt number versus the Reynolds number and the Prandtl number. As shown in Fig. 4, a best fitting plane was passed through the calculated data, where the hollow circles show data placed below the correlated plane and solid circles show data above the correlated plane. The following equation was found to suitably represent the results for the whole Reynolds numbers ranging from 290 to 7480 and the Prandtl numbers from 2.77 to 6.5. The correlation coefficient for this equation is $r^2 = 0.96$.

$$Nu_{D_h} = 0.0155 \mathrm{Re}_{D_h}^{\ 0.955} \mathrm{Pr}^{0.43}, \qquad \begin{cases} 290 < \mathrm{Re} < 7840 \\ 2.77 < \mathrm{Pr} < 6.5 \\ \alpha = 0^\circ \end{cases} \tag{6}$$

The above correlation can also be used for natural circulation system due to very low mass flow rates ranging from 0.0012 to 0.0519 kg/s.

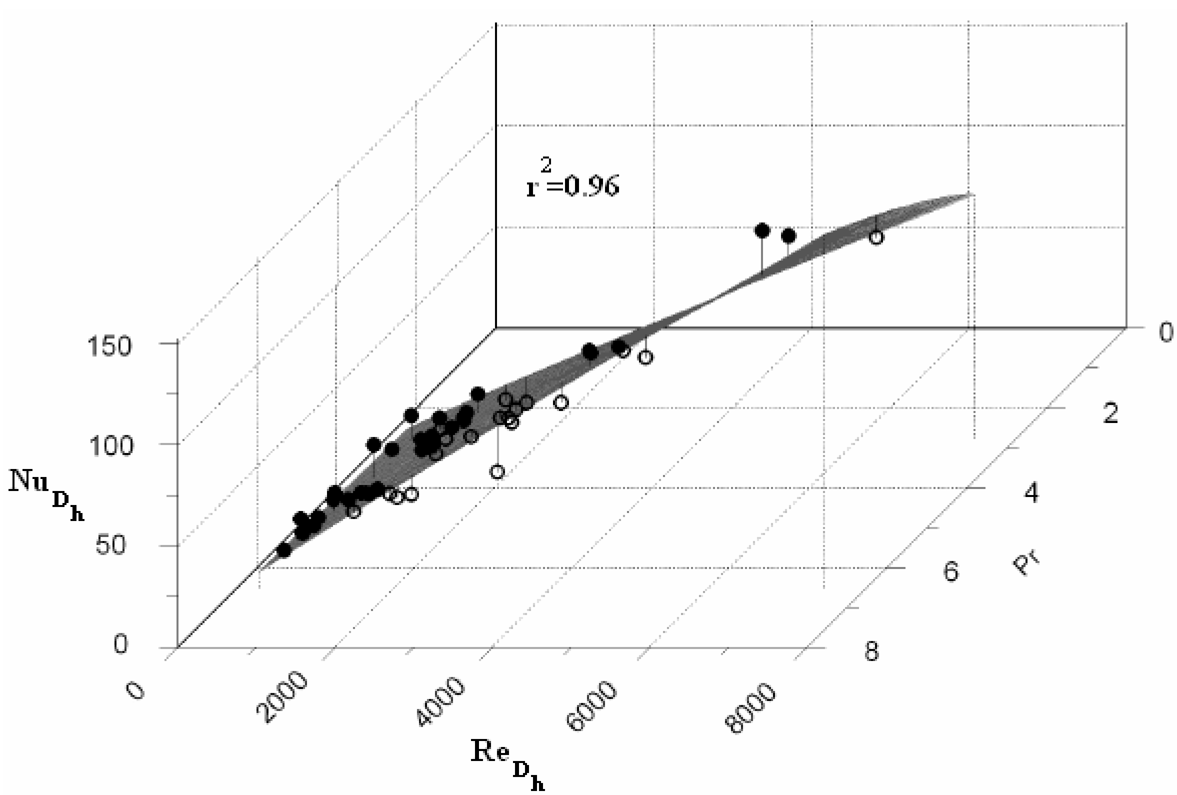

Fig. 4. The Nusselt number versus the Reynolds number and the Prandtl number

TEMPERATURE DISTRIBUTION

The temperature distribution along the finned tube of a flat plate collector for $\mathrm{Re}_{D_h} = 1400$ is shown in Fig. 5 for three values of water inlet temperature. Three temperatures in the diagram show the wall temperatures and the fluid temperature, which for the former two thermocouples were installed at the top and the bottom surface at each point and for the latter; one thermocouple was inserted in the middle of the tube cross-section according to Fig. (2).

It can be seen that at each point the top wall temperature is higher than the bottom wall temperature. In fact, this is due to the secondary flow at each cross-section, which pushes the cold fluid to the bottom surface. The same result was reported by Morcos et al., 1986.

The inlet water temperatures tested were 19, 45 and 55 $^{\circ}C$ and the mass flow rate was 0.0064 kg/s. It is evident from Fig. 5 that for the first two data points, the temperature rise is slower compared to the rest of the points. This is because the flow is developing in the entrance of the tube. It can also be seen that although the heat flux is entering from the top surface of the finned tube, the temperature at the bottom of the tube is still higher than the fluid temperature. This is due to the heat conduction through tube-side walls.

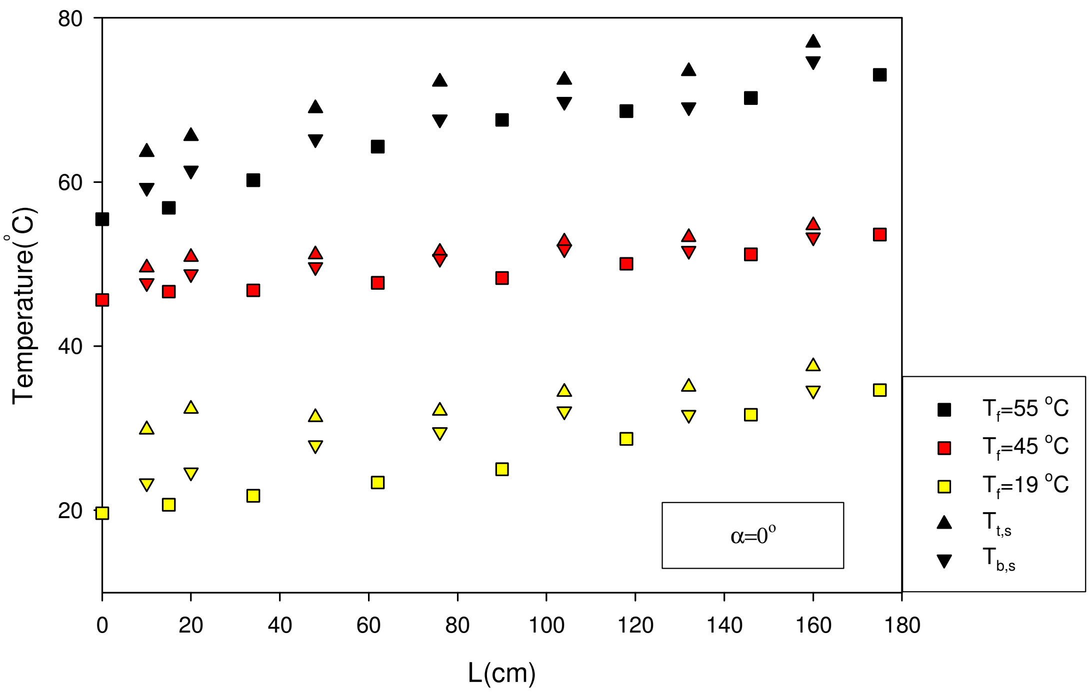

Fig. 5. Temperature distribution along the finned tube for $\mathrm{Re}_{D_h} = 1400$

Fig. 6 shows the temperature distribution for different Reynolds number and for the same water inlet temperature. It is observed as the Reynolds number increases, the temperature rise becomes smaller as expected. The difference between top and bottom surface temperatures is higher for the first points and it reduces as the fluid flows toward the exit. It is due to the developing region, which exists in the inlet area and as the boundary layer grows, the state of fully developed flow is achieved.

CONCLUSIONS

In the current study, a typical horizontal Sunstrip fins was tested for obtaining its heat transfer coefficient in laminar forced-convection flow. Two correlations were proposed for the Nusselt number as a function of the Reynolds number and the Prandtl number based on hydraulic diameter of the rhombic cross-section tube of the flat plate collector. The temperature distribution was also investigated along the finned tube.

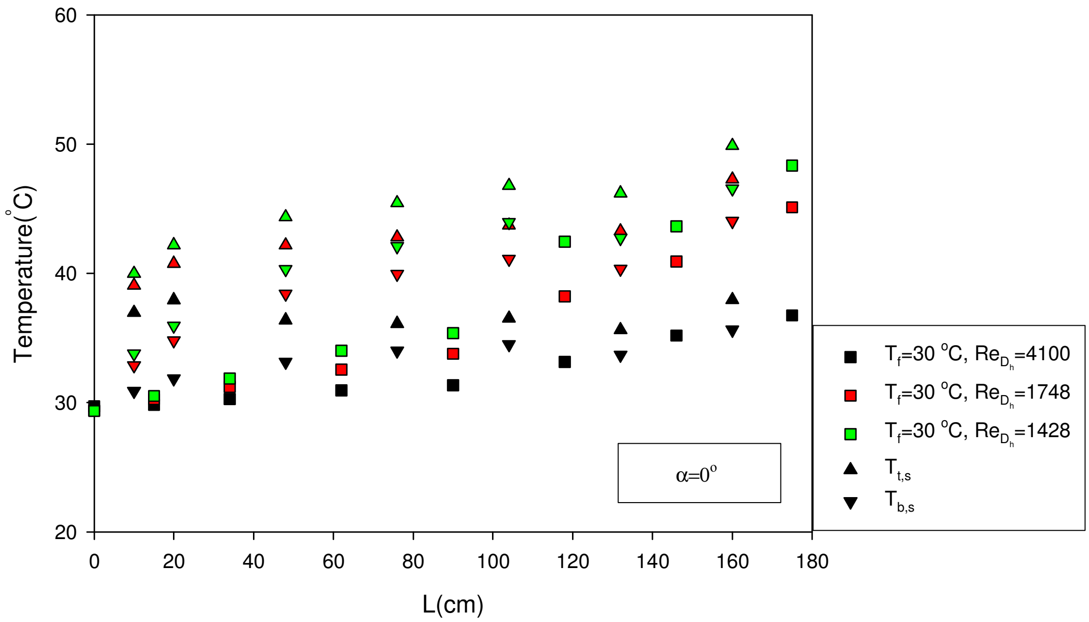

Fig. 6. Temperature distribution for three different Reynolds number at the same inlet temperature

NOMENCLATURE

A	surface area, m^2
C_p	specific heat capacity, $J/kg^{\circ}C$
D	diameter, m
g	gravity acceleration, m/s^2
h	heat transfer coefficient, $W/m^{2\,\circ}C$
L	total length of Sunstrip fin, m
$\dot{m}$	mass flow rate, kg/s
Nu	Nusselt number
$\Pr$	Prandtl number
Q	net heat rate, W
Re	Reynolds number
T	temperature, $^{\circ}C$
V	velocity, m/s

Greek letters

α	Collector tilt
β	Coefficient of thermal expansion, $1/K$
μ	viscosity, Ns/m^2
ρ	density, kg/m^3

Subscript

c	Cross-section
F, f	fluid
i	inlet
m	Mean, average
o	outlet
s	surface, wall

REFRENCES

J. A. Duffie, W. A. Beckman. 1991. *Solar Engineering of Thermal Processes*. New York: John Wiley & Sons

J. P. Chiou. 1982. The effects of nonuniform fluid flow distribution on the thermal performance of solar collector. *Solar Energy* 29:6:487-502.

G. F. Jones, N. L. Lior. 1994. Flow distribution in manifolded solar collectors with negligible buoyancy effects. *Solar Energy* 52:3:289-300.

V. Weitbrecht, D. Lehmann, A. Richter. 2002. Flow distribution in solar collectors with laminar flow conditions. *Solar Energy* 73:6:433-441.

J. Fan, L. J. Shah, S. Furbo. 2005. Flow distribution in a solar collector panel with horizontal fins. *Proceedings ISES Solar World Congress*, Orlando, USA.

S. J. Kline, F. A. McClintock. 1953. Describing uncertainties in a single-sample experiments. *Mechanical Engineering* 75:3-8.

S. M. Morcos, M. M. Hilal, M. M. Kamel, M.S. Soliman. 1986. Experimental investigation of mixed laminar convection in the entrance of inclined rectangular channels. Journal of Heat Transfer 108:574-579.

E. M. Sparrow, A. Haji-Sheikh. 1966. Flow and heat transfer in ducts of arbitrary shape with arbitrary boundary conditions. Journal of Heat Transfer 88:351-358.